

# Parametric synthesis of 3D structure of SRR element of the metamaterial

Ihor Sliusar

Department of information systems and technologies  
Poltava State Agrarian Academy  
Poltava, Ukraine  
islyusar2007@ukr.net

Yurii Utkin

Department of information systems and technologies  
Poltava State Agrarian Academy  
Poltava, Ukraine  
1008utkin@gmail.com

Vadym Slyusar

Central Research Institute of Armaments and Military  
Equipment of Armed Forces of Ukraine  
Kyiv, Ukraine  
swadim@ukr.net

Olena Kopishynska

Department of information systems and technologies  
Poltava State Agrarian Academy  
Poltava, Ukraine  
17elenak@gmail.com

**Abstract**—Variants of split ring resonators (SRR) models are proposed. They are considered as unit cells of DNG metamaterials. The synthesized SRR variants are based on the implementation of 3D geometry. Efficiency assessment is carried out on the base of determination of the relative bandwidth  $\delta f_{DNG}$ , in which the DNG properties are observed. Since metamaterials are complex composite structures, instead of analytical calculations, the Finite Element Method (FEM) is used to estimate the electromagnetic properties of SRR. The adequacy of the proposed SRR model is confirmed by the coincidence of the obtained results in the particular case with the corresponding estimates of the base model. At the same time, the influence of the geometric parameters of the SRR components (orientation and size of the conductor; axial rotation of the rings, subtract material) on the effectiveness of the decisions was investigated. The use of 3D-based constituent elements in SRRs allowed us to achieve a 10 times increase in  $\delta f_{DNG}$  compared to the base prototype.

**Keywords**—double negative; metamaterial; split ring resonator

## I. INTRODUCTION

Telecommunication miniaturization trends have intensified the search for approaches to the creation of Electrically Small Antennas (ESA) [1]. At the same time, the technologies of microstrip antennas have reached their limits in terms of reducing the dimensions of microwave devices. As a result, one of the promising areas of ESA design is the use of metamaterials.

As is known [2, 3], metamaterials as substrates for printed miniature antennas can reduce the size of the emitters, increase their passband and radiation efficiency.

Metamaterials that contain only one negative electromagnetic parameter ( $\epsilon_r$  or  $\mu$ ) are called Single Negative (SNG). However, the greatest interest is shown in the creation of metamaterials with a negative refractive index of electromagnetic waves, which are characterized simultaneously by negative values of the dielectric constant and magnetic permeability ( $\epsilon_r < 0$ ,  $\mu < 0$ ) [2, 3]. Such materials are called Double Negative (DNG) [2, 3].

At the same time, the main task of improving of the metastructures is the synthesis of such environment that

would have minimal losses and almost insignificant dispersion properties, as well as provide a wide frequency band corresponding to DNG.

## II. ANALYSIS OF RECENT STUDIES AND PUBLICATIONS, WHICH DISCUSS THE PROBLEM

To identify a metamaterial as a DNG, it is necessary to evaluate its electromagnetic properties. Such an estimate comes down to an analysis of the sign of the real part of the quantities  $\epsilon_r$  and  $\mu$ . The following relations should be used [4]:

$$\epsilon_r = n / z \text{ и } \mu = n \cdot z, \quad (1)$$

where  $n$  is the refractive index;  $z$  is the wave impedance.

In turn, to obtain the values of  $n$  and  $z$ , you can use the formulas [5]:

$$n = \frac{1}{k_0 d} \arccos \left[ \frac{1}{2S_{21}} (1 - S_{11}^2 - S_{21}^2) \right], \quad (2)$$

$$z = \sqrt{\frac{(1 + S_{11})^2 - S_{21}^2}{(1 - S_{11})^2 - S_{21}^2}}, \quad (3)$$

where  $k_0 = 2\pi f/c$ ,  $c$  – speed of light,  $f$  – frequency,  $d$  – linear size of the metamaterial unit cell,  $S_{xy}$  – S-parameters of dispersion matrix [5].

As a classic example of the metastructure unit cell, on the basis of which a negative refractive index can be achieved (accordingly, a DNG frequency range can exist), the Split Ring Resonator (SRR) should be mentioned [2, 3]. Such a structure is described more in detail in [6].

The systematization of existing sources related to this topic indicates that the studies of the joint use of microstrip or patch antennas and metamaterials are dominant [4, 7-11].

Unfortunately, metamaterials based on circular or rectangular SRRs are characterized by a narrow DNG frequency band, high level of electromagnetic losses, etc [6]. To make up for flaws, it is possible to form structures,

in which perpendicular arrangement of metamaterial cells based on printed SRRs is used [12] or several layers based on them [6] are implemented.

However, to reveal all the possibilities for integrating ESA technologies and metamaterials, it is advisable to conduct an open optimization of the parameters of SRR structural elements, for example, through the use of 3D geometry. A similarity of such structures may be a design option from [13].

Considering that metamaterials are complex composite structures, analytical solutions to assess their properties become inapplicable. As a result, the role of fixed assets in the process of metamaterials designing is assigned to numerical modeling. In this case, the most common is the use of the Finite Element Method (FEM), successfully tested by the authors, for example, in [14-16].

### III. THE AIM OF RESEARCH

Thus, the aim of the work is to increase the efficiency of metamaterial using SRR by modifying its geometry.

### IV. THE MAIN RESULTS OF THE STUDY

In this paper, a printed SRR [7] was used as a prototype, the model of which is presented in HFSS [7, 17] – Fig. 1.

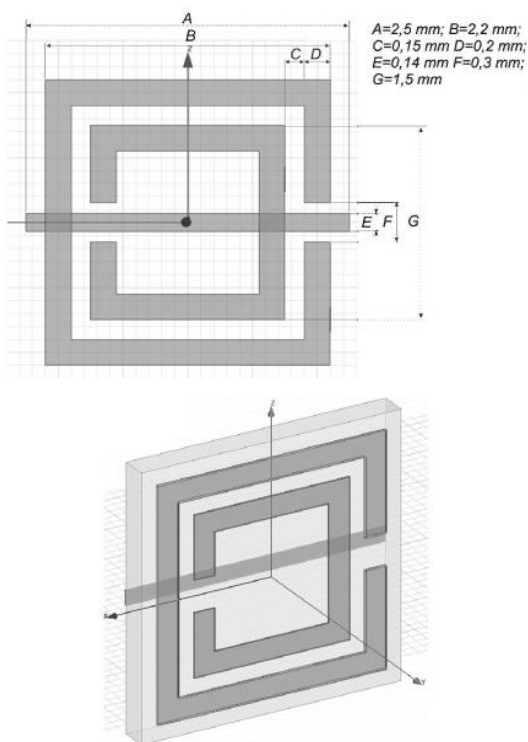


Fig. 1. Printed SRR as a base model.

The indicated SRR variant contains a composite epoxy material substrate (in HFSS this material is FR4). On one of its surfaces there are metal split “rings”, and on the other – conductor. Since the model of such an SRR is one unit cell, which should be in a multi-element system, the formation of limit conditions in the form of a “Master / Slave” boundary on the x- and y-edges of the model will be most acceptable (Fig. 2.a) [7]. This area is very critical for determining the correct location of the excitation ports,

which should be located quite far from the near fields induced on the SRR structure. This ensures that the dispersion parameters are calculated correctly. Since the exact calculation of the S-parameter phase is important for an efficient parameter estimation [7], the ports are displayed on the inner surface of the box describing the boundary conditions (blue arrows in Fig. 2.b). Herein, a modification of wave ports is used, which is called “Floquet Ports” [7], since in these ports the harmonics of Floquet with zero indices propagates (it is often called the main harmonics). It has a field structure that matches the field of the incident wave. In this case, higher order harmonics are not excited.

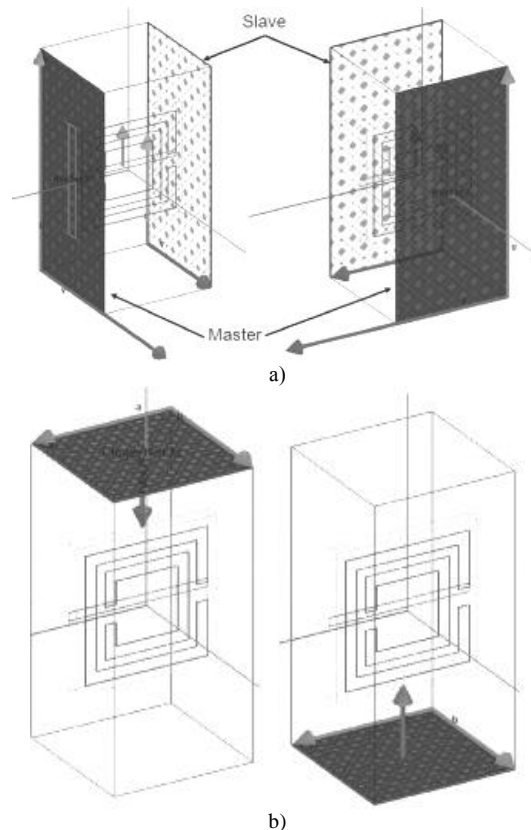


Fig. 2. Formation of the calculation area: a) – “Master / Slave” boundary conditions; b) – Floquet Ports [7].

Based on the considered model, the authors synthesized the SRR variant based on the implementation of 3D geometry (Fig. 3). The following situations were considered as introduced assumptions:

- SRR “rings” and conductor made of copper; the orientation of the wire and the cuts of the “rings” of the SRR are identical to the base model;
- the geometric dimensions of the SRR components according to Ox and Oz coincide with the same parameters of the base model;
- subject to change – the dimensions of the SRR components along the Oy axis;
- to correctly compare the properties of the basic and synthesized SRR models, its dimensions should not extend beyond the figure (parallelepiped) describing the boundary conditions of the basic model;
- analysis is carried out in the range 0.1 ÷ 20 GHz;

- conditions for the calculations coincide with the base model;
- performance assessment is based on determining the relative bandwidth, for which the conditions  $\epsilon_r < 0$ ,  $\mu < 0$  are valid.

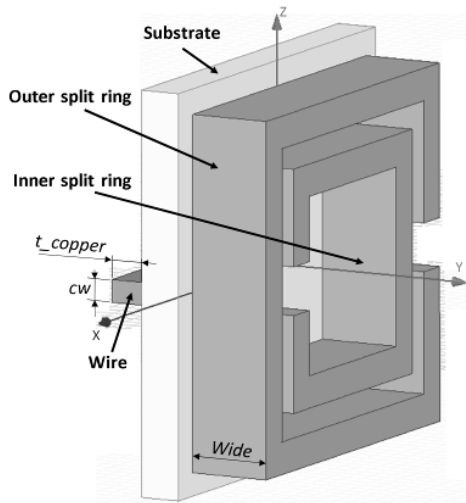


Fig. 3. Synthesized model No. 1 of metamaterial cell.

There are several options for interpreting of the concept of “relative bandwidth”. Following [14, 15], we further use the definition that corresponds to the expression:

$$\delta f_{DNG} = \frac{2|\Delta f|}{f_1 + f_2}, \quad (4)$$

where  $f_1$  and  $f_2$  are the limit values of the frequencies of the range characterized by the condition:  $\{\text{Re}(\epsilon_r) < 0 \text{ and } \text{Re}(\mu) < 0\}$ ,  $\Delta f = f_2 - f_1$ .

To check the adequacy of the proposed model No. 1 (Fig. 3) with respect to the base, the substrate material “FR4 epoxy” ( $\epsilon_r = 4.4$ ) was selected and the first calculation was carried out with the values of the variables:  $t_{copper} = \text{Wide} = 0,017$  mm. The results obtained coincided with the corresponding estimates of the base model ( $\delta f_{DNG} = 0.19$ ). At the same time, a new graph (Fig. 4) was formed as the result, which shows the frequency dependences of  $\text{Re}(\epsilon_r)$  and  $\text{Re}(\mu)$ .

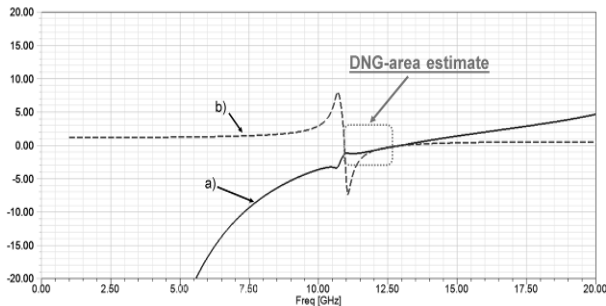


Fig. 4 Evaluation of the characteristics of model SRR No. 1: a) –  $\text{Re}(\epsilon_r)$ ; b) –  $\text{Re}(\mu)$ .

Further, the dependence of  $\delta f_{DNG}$  on the geometric dimensions of the conductor and SRR rings along the Oy axis was studied. First, the situation of a synchronous increase in their size was considered (Table I), and then the size of the SRR rings was fixed and the dimensions of the conductor were changed along the Oy axis. The corresponding results are presented in Table II. The greatest effect is observed at  $t_{copper} = \text{Wide} = 1$  mm, for

which  $\delta f_{DNG} = 0.335$  was obtained (Fig. 5). It can be assumed that a further increase in the size of the cell will lead to the expansion of the DNG region.

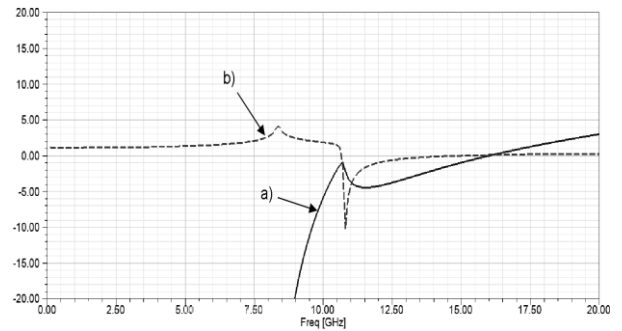


Fig. 5. DNG SRR estimate at  $t_{copper} = \text{Wide} = 1$  mm: a) –  $\text{Re}(\epsilon_r)$ ; b) –  $\text{Re}(\mu)$ .

The analysis indicates an increase in the width of the DNG frequency range as the dimensions of the SRR constituent elements along the Oy axis increase.

TABLE I. DNG BANDWIDTH ESTIMATION

Variable structures, mm		Boundary frequencies, GHz		Bandwidth	
$t_{copper}$	Wide	$f_1$	$f_2$	$\Delta f$ , GHz	$\delta f_{DNG}$
0.017	0.017	12.32	14.30	1.98	0.149
0.0358	0.0358	12.32	14.30	1.98	0.149
0.1	0.1	12.17	14.70	2.53	0.19
0.2	0.2	11.92	14.89	2.97	0.222
0.3	0.3	11.73	14.89	3.16	0.237
0.4	0.4	11.51	14.86	3.35	0.254
0.5	0.5	11.34	14.86	3.52	0.269
0.6	0.6	11.21	14.92	3.71	0.284
0.7	0.7	11.04	14.89	3.85	0.297
0.8	0.8	10.92	14.97	4.05	0.313
0.9	0.9	10.78	14.97	4.19	0.325
1	1	10.67	14.97	4.3	0.335

TABLE II. THE RESULTS OF CALCULATIONS OF THE FREQUENCY DOMAIN DNG WHEN CHANGING THE SIZE OF THE CONDUCTOR AND FIXING THE SIZE OF THE SRR RINGS ALONG THE AXIS OY

Variable structures, mm		Boundary frequencies, GHz		Bandwidth	
$t_{copper}$	Wide	$f_1$	$f_2$	$\Delta f$ , GHz	$\delta f_{DNG}$
0.1	0.7	11.33	12.22	0.89	0.076
0.2		11.26	12.96	1.7	0.14
0.4		11.20	14.13	2.93	0.213
0.6		11.10	14.86	3.76	0.29

The next step in the study was to assess the effect of the substrate material. In addition to the classic FR4, several material options were considered: Rogers RO3003 ( $\epsilon_r = 3$ ); Rogers RO3006 ( $\epsilon_r = 6.15$ ); Rogers RO3010 ( $\epsilon_r = 10.2$ ); and vacuum. By the way, using of vacuum as the substrate material allows us to transform model No. 1 to the variant shown in Fig. 6.

Herein, the values of the variables  $t_{copper} = \text{Wide} = 0.2$  mm were taken. Corresponding estimates of the length of the DNG frequency domain are shown in Fig. 7-10 and are presented in Table III.

The obtained results suggest the possibility of a slight decrease in the frequency range of the DNG domain due to the use of a substrate material with a higher  $\epsilon_r$  value.

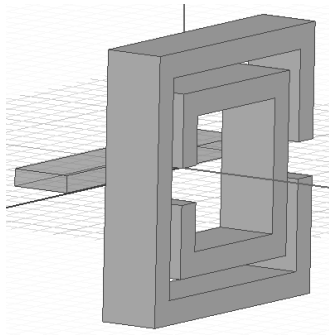


Fig. 6. Version of the model SRR without substrate.

TABLE III. ESTIMATION OF THE DNG FREQUENCY DOMAIN WHEN THE SRR SUBSTRATE MATERIAL CHANGES

Material ( $\epsilon_r$ )	Variable structures, mm		Boundary frequencies, GHz		Bandwidth	
	$t_{copper}$	Wide	$f_1$	$f_2$	$\Delta f$ , GHz	$\delta f_{DNG}$
Vacuum (1)	0.2	0.2	14.10	17.59	3.49	0.22
RO3000 (tm) (3)	0.2	0.2	12.61	15.71	3.1	0.22
FR4_epoxy (4.4)	0.2	0.2	11.92	14.89	2.97	0.22
RO3006 (tm) (6.15)	0.2	0.2	11.45	14.22	2.77	0.22
RO3010 (tm) (10.2)	0.2	0.2	10.63	12.94	2.31	0.2

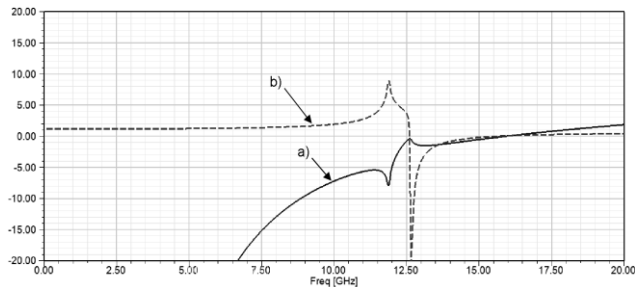


Fig. 7. Estimation of the DNG frequency domain for the Rogers RO3003 substrate material: a) –  $Re(\epsilon_r)$ ; b) –  $Re(\mu)$ .

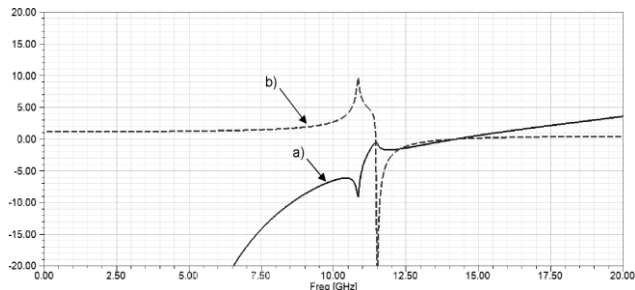


Fig. 8. Estimation of the DNG frequency domain for the Rogers RO3006 substrate material: a) –  $Re(\epsilon_r)$ ; b) –  $Re(\mu)$ .

Considering the presence of an SRR modification without a substrate (see Fig. 6), it is advisable to analyze the influence of the angle of inclination of the SRR rings around the Ox axis on the frequency properties of the metamaterial unit cell model (Fig. 11) for the same variables:  $t_{copper} = Wide = 0.2$  mm. It is significant that an increase in these values may lead to contact between the SRR rings, which is unacceptable. The research results were systematized and summarized in Table IV. Thus, the inclination of the SRR rings around the Ox axis did not give a significant improvement in the properties of the

metamaterial cell according to the maximum criterion  $\delta f_{DNG}$ .

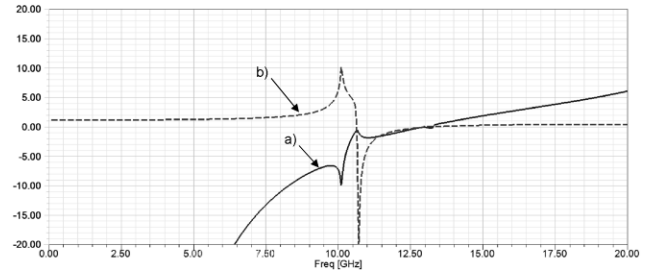


Fig. 9. Estimation of the DNG frequency domain for the Rogers RO3010 substrate material: a) –  $Re(\epsilon_r)$ ; b) –  $Re(\mu)$ .

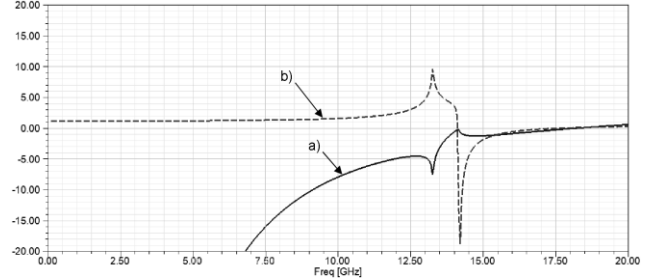


Fig. 10. Estimation of the DNG frequency domain for the model shown in Fig. 6: a) –  $Re(\epsilon_r)$ ; b) –  $Re(\mu)$ .

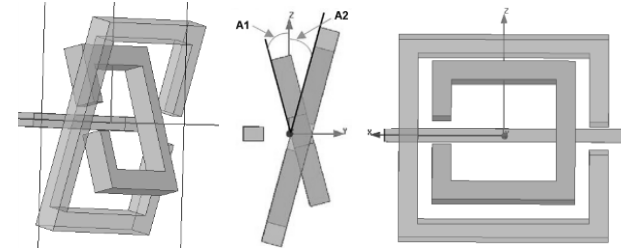


Fig. 11. Model No. 2, with AN option of independent selection of the angle of inclination of the outer and inner rings of the SRR.

TABLE IV. RESULTS OF CALCULATIONS OF THE FREQUENCY AREA DNG WHEN CHANGING AN ANGLE OF THE RINGS SRR AROUND THE OX AXIS

Angles of inclination, deg		Variable structures, mm		Boundary frequencies, GHz		Bandwidth	
A1	A2	$t_{copper}$	Wide	$f_1$	$f_2$	$\Delta f$	$\delta f_{DNG}$
0	0	0.2	0.2	13.92	18.06	4.14	0.259
4	0	0.2	0.2	13.47	17.52	4.05	0.261
5	0	0.2	0.2	13.96	18.19	4.23	0.263
10	0	0.2	0.2	14.07	18.15	4.08	0.253
0	-5	0.2	0.2	14.03	17.99	3.96	0.247
0	5	0.2	0.2	14.03	17.99	3.96	0.247
5	5	0.2	0.2	14.16	17.99	3.83	0.238
15	-15	0.2	0.2	15.31	17.61	2.3	0.14
-15	15	0.2	0.2	15.51	17.07	1.56	0.096
5	-5	0.5	0.2	13.86	18.12	4.26	0.267

A further area of research was the determination of the influence of the orientation of the conductor relative to the SRR rings. At the same time, it was located in the xOy plane, and it rotated around the Oz axis by 90 degrees (Fig. 12). This approach has led to an expansion in bandwidth in the DNG region (Fig. 13), which indicates its effectiveness. In this case, the value  $\Delta f = 8.64$  GHz ( $\delta f_{DNG} = 1.13$ ) was achieved. For a given SRR arrangement in Fig. 14 shows the frequency dependence of  $Re(n)$ .

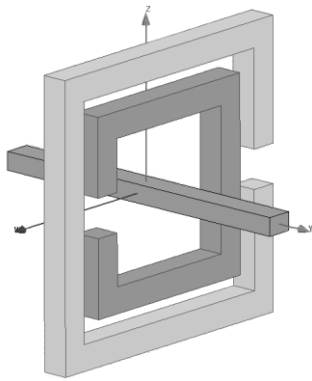


Fig. 12. Model SRR No. 3.

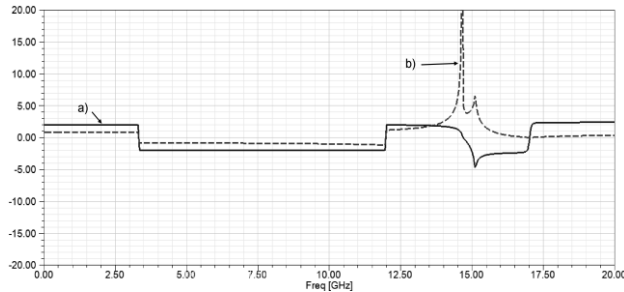


Fig. 13. Assessment of the DNG frequency domain for model No. 3: a) –  $\text{Re}(\epsilon_r)$ ; b) –  $\text{Re}(\mu)$ .

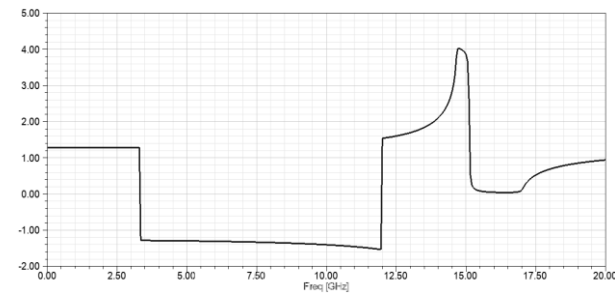


Fig. 14. Evaluation of the real component of the refractive index  $\text{Re}(n)$  for model No. 3.

Hereinafter, we analyzed the influence of changes in the dimensions of the conductor, its placement in relation to the center of the SRR, as well as the previously considered versions of the SRR models, but taking into account the changed spatial orientation of the conductor.

In addition, the SRR model was investigated with rings rotated by 90 degrees around the Oy axis (Fig. 15), with sections of the SRR frames located on the Oz axis. This allowed us to obtain  $\Delta f = 10.78$  GHz and  $\delta f_{DNG} = 1.9$  (Fig. 16).

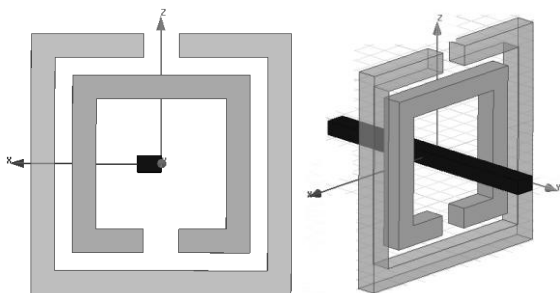


Fig. 15. Model SRR No. 4.

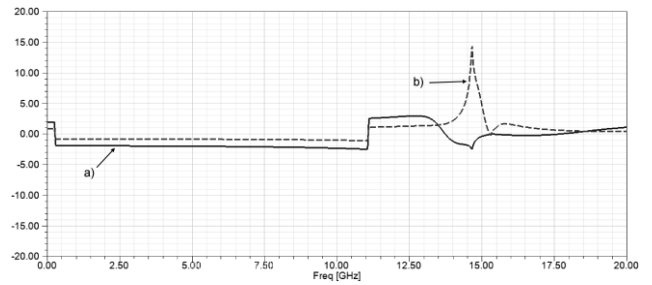


Fig. 16. Assessment of the frequency domain DNG for model No. 4: a) –  $\text{Re}(\epsilon_r)$ ; b) –  $\text{Re}(\mu)$ .

Considering an obtained effect, the SRR layout option was studied in the most detail, which differed by the deviation of the rings section in relation to the Oz axis by angles of up to  $\pm 30$  degrees (Fig. 17). In this case, fluctuations in the value of  $\delta f_{DNG}$  occurred. As a result, the maximum effect was observed at the deviation angle of 20 degrees (Fig. 18).

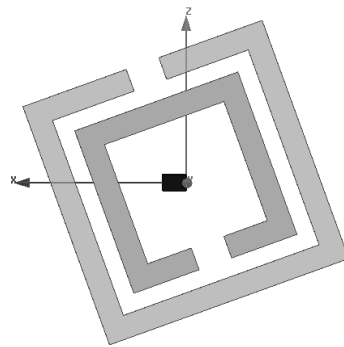


Fig. 17. Model SRR No. 4 (with variation of the inclination angle of the rings rupture in relation to the axis Oz).

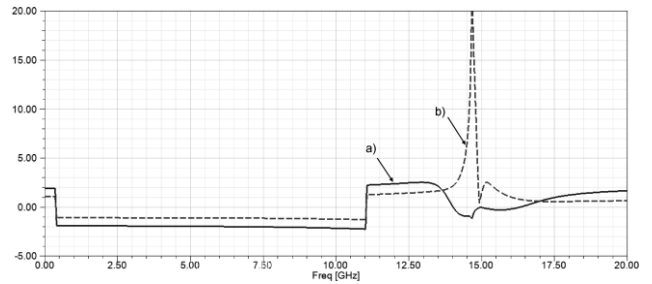


Fig. 18. Assessment of the DNG frequency domain for model No. 4 with an inclination angle of the cut of rings 20 degrees: a) –  $\text{Re}(\epsilon_r)$ ; b) –  $\text{Re}(\mu)$ .

To increase  $\Delta f$ , it is possible to introduce mutual rotation of SRR rings around the Oz axis. For instance, for the model shown in Fig. 19, this made it possible to provide an additional increment of  $\Delta f$  at 0.5 GHz.

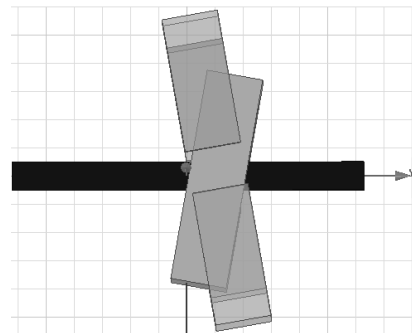


Fig. 19. SRR with mutual rotation of the rings around the axis Oz (top view).

In general, the estimates of the synthesized SRR models allow us to conclude that for the expansion of the DNG frequency regions and their simultaneous shift down in frequency, it is advisable to perform mutual displacement between the SRR rings. However, it should be considered that such a shift is acceptable only within certain limits.

#### V. PERSPECTIVES OF FURTHER RESEARCH

It is advisable to focus further research on studying of the electromagnetic parameters of SRR structures, in which the constituent elements are modeled on the basis of fractals [18] or antifractals.

Another direction of designing such SRRs may be the combination of square frames and round rings, as well as the introduction of various types of dielectric inserts into the SRR, which are based on dielectric resonator antenna technologies [16].

#### VI. CONCLUSIONS

The study of the electromagnetic properties of the synthesized SRR variants was carried out taking into account the influence of geometric parameters (orientation and size of the conductor; axial rotation of the rings, substrate material).

Compared with the prototype [7], the synthesized SRR models allow one to obtain a 10-fold increase in  $\delta f_{DNG}$  c 0.19 to  $\approx 1.9$ .

SRR with the conductor placed in the xOy plane and its axis oriented perpendicular to xOz is an effective solution that has led to the expansion of the DNG bandwidth in the low frequency region.

The use of a conductor with a rectangular cross section is advisable if its larger side is oriented perpendicular to the Floquet Ports.

When determining the optimal angle of inclination of the section plane of the SRR frames in relation to the yOz plane, it is advisable to choose it within the range of  $0 \div 90$  degrees.

If we consider the synthesized SRR model as a template for creating a metastructure, then the cut width of the frames should be equal to the double thickness of the rings.

To expand the frequency domain of the DNG and simultaneously shift it down in frequency, it is advisable to perform a mutual offset between the SRR rings. However, it should be considered that it only makes sense to do this within certain limits.

#### REFERENCES

- [1] V.I. Slyusar "60 Years of Electrically Small Antennas Theory", in *IEEE 2007 6th International Conference on Antenna Theory and Techniques*, Sevastopol, 2007, pp. 116-118, DOI: <https://doi.org/10.1109/ICATT.2007.4425129>.
- [2] V.I. Slyusar "Metamaterials on antenna solutions", in *IEEE 2009 7th International Conference on Antenna Theory and Techniques (ICATT'09)*, Lviv, 2009, pp. 19-24.
- [3] V.I. Slyusar "Metamaterialy v antennoj technique: osnovnyye principy i rezultaty" [*Metamaterials in the antenna equipment: basic principles and results*] *The First Mile (Pervaya milya)*, 2010, vol. 3, 4, pp. 44-60. (In Russian).
- [4] D.R. Smith, D.C. Vier, Th. Koschny and C.M. Soukoulis "Electromagnetic parameter retrieval from inhomogeneous metamaterials", *The American Physical Society. Physical Review E* 71, 036617 s2005d, DOI: <https://doi.org/10.1103/PhysRevE.71.036617>.
- [5] S.E. Bankov, E.M. Gutzajt and A.A. Kurushin, *Reschenie opticheskikh i SVCH zadach s pomoshchyu HFSS [Solving optical and microwave problems using HFSS.]* – Moscow, Russia: OOO "Orcada", 2012, 250 p. (In Russian).
- [6] J.B. Pendry et al. "Magnetism from conductors and enhanced nonlinear phenomena", *IEEE Trans. Microw. Theory Tech.*, 1999, vol 47, pp. 2075-2081.
- [7] Ansys, "3D Electromagnetic Field Simulator for RF and Wireless Design" [Online]. Available: <https://www.ansys.com/products/electronics/ansys-hfss>. [Accessed 15 July 2020].
- [8] S. Nanda, D. De, P.K. Sahu and R.K. Mishra "Metamaterial synthesis using a CAD model based on an evolutionary technique to improve the performance of TCAS antennas", *Journal of Computational Electronics*, 2019, vol. 18, pp. 1291-1305, DOI: <https://doi.org/10.1007/s10825-019-01367-7>.
- [9] S.S. Seetharaman, I.R. Hooper, and W.L. Barnes "Metamaterial Analogues of Molecular Aggregates Milo Baraclough", *ACS Photonics*, 2019, vol. 6 (11), pp. 3003-3009, DOI: <https://doi.org/10.1021/acsphotonics.9b01208>.
- [10] J.J. Paul and A.S. Rekh "Study and Analysis of Various SRR Patch Structures for Energy Harvesting Applications", in *2020 5th International Conference on Communication and Electronics Systems (ICCES)*, Coimbatore, 2020, pp. 326-329, DOI: <https://doi.org/10.1109/ICCES48766.2020.9138062>.
- [11] M.-F. Wu et. al. "Miniaturization of a Patch Antenna with Dispersive Double Negative Medium Substrates", in *IEEE 2005 Asia-Pacific Conference Microwave Proceedings (APMC 2005)*, China, [Online]. Available: <https://ieeexplore.ieee.org/document/1606177/authors#authors>. [Accessed 15 July 2020].
- [12] C.T. Chevalier and J.D. Wilson "Frequency Bandwidth Optimization of Left-Handed Metamaterial", *NASA/TM-2004-213403*, November 2004. [Online]. Available: <https://ntrs.nasa.gov/archive/nasa/casi.ntrs.nasa.gov/20050019217.pdf>. [Accessed 15 July 2020].
- [13] Z. Jaksic, M. Maksimovic and N. Dalarsson "Negative Refractive Index Metamaterials: Principles and Applications" *Microwave Review*, Jun 2006, pp. 36-49.
- [14] I.I. Sliusar, V.I. Slyusar, S.V. Voloshko, A.O. Zinchenko and L.N. Degtyareva "Synthesis of quasi-fractal ring antennas", in *IEEE 2019 6th International ScientificPractical Conference Problems of Infocommunications. Science and Technology (PIC S&T)*, Kyiv, 2019, pp. 741-744, DOI: <https://doi.org/10.1109/PICST47496.2019.9061286>.
- [15] I.I. Sliusar, V.I. Slyusar, S.V. Voloshko and L.N. Degtyareva "Antenna synthesis based on fractal approach and DRA technologies", in *IEEE 2th Ukraine Conference on Electrical and Computer Engineering (UKRCON-2019)*, Lviv, 2019, pp. 29-34, DOI: <https://doi.org/10.1109/UKRCON.2019.8879953>.
- [16] I.I. Sliusar, V.I. Slyusar, S.V. Voloshko and V.G. Smolyar "Synthesis of quasi-fractal hemispherical dielectric resonator antennas", in *IEEE 2018 5th International ScientificPractical Conference Problems of Infocommunications. Science and Technology (PIC S&T)*, Kharkov, 2018, pp. 313-316, DOI: <https://doi.org/10.1109/INFOCOMMST.2018.8632087>.
- [17] S.E. Bankov and A.A. Kurushin, *Raschet antenn i SVCH struktur s pomoshchyu HFSS Ansoft [Calculation of antennas and microwave structures using HFSS Ansoft]*, Moscow, Russia: ZAO NPP "Rodnik", 2009, 736 p. (In Russian).
- [18] B. Mandelbrot, *Fractals: Forme, Chance and Dimension*. San-Francisco, Freeman, 1977, 365 p.